A NEW ERA OF EXPLORATION OF LUNAR ALPHONSUS CRATER. Lisa R. Gaddis[1], Trent Hare[1], Samuel Lawrence[2], Julie Stopar[2], Jim Skinner[1], Justin Hagerty[1], [1]Astrogeology Science Center, U. S. Geological Survey, 2255 North Gemini Drive, Flagstaff, AZ 86001; [2]School of Earth and Space Exploration, Arizona State University, Tempe, AZ 85282 (lgaddis@usgs.gov).

Introduction: Dark-halo craters in Alphonsus crater (108 km diameter; ~13°S/357°E) are considered type localities of small lunar pyroclastic deposits (***Figure 1***), based on the observed association of dark mantling material with floor fractures, non-circular craters, and positive-relief features marking source vents. The Alphonsus pyroclastic deposits have been of high interest for decades, in part because of reports of possible degassing or "transient lunar phenomena" events observed from Earth [1-3] and the possibility of active volcanism there. Ranger 9 obtained detailed photographs of the crater floor prior to crashing northeast of the central peak [4] and the crater floor was considered as a possible landing site for both Apollo missions 16 and 17 [5, 6]. In this analysis, we present recent remote sensing data that lend support for Alphonsus as a future lunar landing site.

Rationale: Head and Wilson [7] mapped the pyroclastic deposits of Alphonsus, and they concluded that juvenile volcanic materials likely were present in many of them. Pyroclastic materials may include the best examples of primitive components (i.e., mantle xenoliths) on the Moon and thus are important for characterizing the lunar interior and constraining the origin and evolution of lunar basaltic magmatism. Volcanic landforms such as those in Alphonsus may represent surface deposits of deep-seated and/or primitive lunar magmas that are accessible for future lunar landed exploration and sample collection.

Earth-based spectral data indicate that the Alphonsus pyroclastic deposits are compositionally diverse and that olivine may be present in several of the pyroclastic deposits [8, 9]. Although more recent research suggested that olivine is likely not present at Alphonsus [10, 11], the iron-rich glasses observed there may provide an invaluable feedstock for lunar oxygen production [12]. In-situ oxygen production is essential for future human exploration and habitation of the Moon [13].

Geologic Setting: Alphonsus is a pre-Imbrian aged crater located in the highlands east of Mare Nubium. Alphonsus has a broad, low rim, a flat cratered floor dissected into eastern and western sections by a ~N-S ridge (likely comprised of Imbrium basin ejecta), and a central peak. The crater floor is covered with a light plains unit that is dissected by numerous floor fractures. The 13 pyroclastic deposits of Alphonsus [14] are located within or adjacent to several floor fractures, indicating that fractures likely provided conduits for volatile accumulation and subsequent pyroclastic eruption. The vents are characterized by non-circular rims <3 km across and dark halos that extend up to 11 km from the crater center [14]. Head and Wilson [7] modeled the eruption of these small pyroclastic deposits as vulcanian, occurring via the accumulation and explosive decompression of volatiles that collected beneath a caprock above a rising magma body.

Accessibility and Traversability: Numerous authors have described science and engineering requirements for lunar traverses at sites of high scientific interest such as Alphonsus [14-19]. Recently available remote sensing data provide a new view of the morphologic, compositional, and physical characteristics of Alphonsus crater and allow us to re-assess the accessibility and traversability of pyroclastic deposits for in-situ exploration. These data include (***Figure 1***): SELENE Kaguya Multiband Imager (MI) at 5 UVVIS wavelengths and ~17 m/pixel (415, 750, 900, 950, 1000 nm; [20]); a topographic model [SLDEM; 21] from merged Kaguya Terrain Camera (TC) and Lunar Reconnaissance Orbiter (LRO) laser altimeter with a horizontal resolution of ~60 m and a vertical accuracy of ~4 m; and a LRO Diviner derived rock abundance image [22]. MI color data allow us to map in detail the location and extent of 13 dark, iron-rich pyroclastic deposits. The SLDEM reveals the distribution of ridges and hummocks, floor fractures and impact craters that might impede trafficability and highlight the ~flat light plains unit of the crater floor. Although the N-S ridge may require that any surface exploration concentrate on either the eastern or western pyroclastic deposits, a slope map (derived from the SLDEM) shows that (at the LOLA scale) the average slope of the flanks on Alphonsus vents is ~4°, with a range between 2° and 8°. Finally, the rock abundance map shows a smooth, unblocky surface over most of the crater floor adjacent to the pyroclastic deposits.

Together, these recent data and derived products for Alphonsus crater show that morphologic and topographic information support exploration of deposits of juvenile volcanic materials. Future work will include mapping of potential hazards in the crater floor, with emphasis on assessment of local and regional slopes, hazards associated with impact crater ejecta deposits and rims, and high-resolution mapping of possible landing sites and

traverses that ensure access to pyroclastic eruption sites within the floor of Alphonsus crater.

References: [1] Alter, D. (1957) Pub. Astron. Soc. Pacific 69, 158. [2] Alter, D. (1959) Pub. Astron. Soc. Pacific 71, 46. [3] Kozyrev, N.A. (1962) The Moon, IAU Symp. 14, 263-272. [4] Hall, R.C. (1977) NASA SP-4210. [5] Binder, A.B & D.L. Roberts (1970) NASA Report P-30. [6] Trask, N.J. (1972) USGS Prof. Paper 599-J. [7] Head, J.W. & L. Wilson (1979) PLPSC 10th, 2861. [8] Hawke et al. (1989) PLPSC 19th, 255. [9] Coombs et al. (1990) PLPSC. 20th, 339. [10] Besse et al. (2014) J. Geophys. Res. Planets 119, 355–372, doi:10.1002/2013JE004537. [11] Jawin et al. (2015) J. Geophys. Res. Planets 120, doi:10.1002/2014JE004759. [12] Allen, C. (2015) 46th LPSC, abs. 1140. [13] Spudis, P.D. & T. Lavoie (2011), 2011 LEAG Mtg, abs. 2021. [14] Gaddis et al. (2011) LPSC 42, abs 2691. [15] Stanley et al. (1967) NASA TM X-53647, 103-108. [16] Bleacher et al. (2008), NLSI Lun. Sci. Conf., abs. 2166. [17] Stopar et al. (2013) 2013 LEAG, abs. 7038. [18] Speyerer et al. (2013) LPSC 44, abs. 1745. [19] Lawrence et al. (2014) LPSC 45, abs. 2785. [20] Ohtake et al. (2008) Earth Planet. Sci. 60, 257-264. [21] Barker et al. (2015) Icarus, in press. [22] Bandfield et al. (2011) J. Geophys. Res. 116, E00H02, doi:10.1029/2011JE003866.

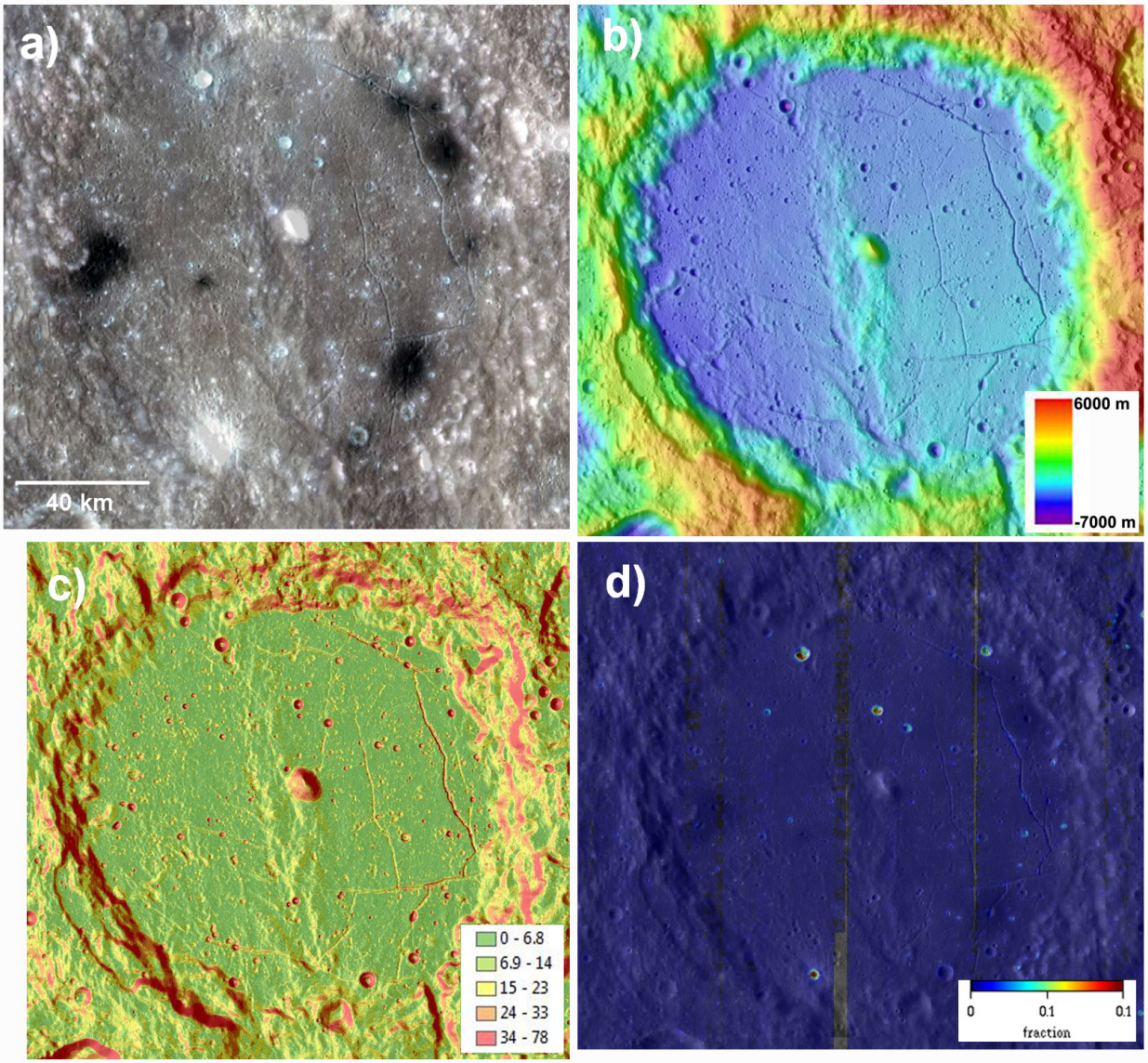

Figure 1. *Views of Alphonsus crater: A) Kaguya* ***MI color mosaic*** *(R=900 nm, G=750 nm, B=415 nm) showing 13 dark pyroclastic deposits. B)* ***Topography*** *(colorized Kaguya TC and LRO LOLA merged map). C)* ***Slope map*** *(in degrees) derived from B, showing the abundant, low-slope (green) terrain of the crater floor. D) Diviner* ***Rock Abundance*** *image, showing a smooth, unblocky surface over most of the crater floor.*